Biochimica et Biophysica Acta 1838 (2014) 413–418

Contents lists available at ScienceDirect

Biochimica et Biophysica Acta

journal homepage: www.elsevier.com/locate/bbamem

Investigating the interaction between peptides of the amphipathic helix of Hcf106 and the phospholipid bilayer by solid-state NMR spectroscopy

Lei Zhang [a], Lishan Liu [a], Sergey Maltsev [a,1], Gary A. Lorigan [a,b], Carole Dabney-Smith [a,b,*]

[a] Department of Chemistry and Biochemistry, Miami University, Oxford, OH 45056, USA
[b] Cell, Molecular, and Structural Biology Graduate Program, Miami University, Oxford, OH 45056, USA

ARTICLE INFO

Article history:
Received 12 March 2013
Received in revised form 1 October 2013
Accepted 4 October 2013
Available online 19 October 2013

Keywords:
Amphipathic helix
Membrane active peptide
Twin arginine transport
Chloroplast TatB

ABSTRACT

The chloroplast twin arginine translocation (cpTat) system transports highly folded precursor proteins into the thylakoid lumen using the protonmotive force as its only energy source. Hcf106, as one of the core components of the cpTat system, is part of the precursor receptor complex and functions in the initial precursor-binding step. Hcf106 is predicted to contain a single amino terminal transmembrane domain followed by a Pro-Gly hinge, a predicted amphipathic α-helix (APH), and a loosely structured carboxy terminus. Hcf106 has been shown biochemically to insert spontaneously into thylakoid membranes. To better understand the membrane active capabilities of Hcf106, we used solid-state NMR spectroscopy to investigate those properties of the APH. In this study, synthesized peptides of the predicted Hcf106 APH (amino acids 28–65) were incorporated at increasing mol.% into 1-palmitoyl-2-oleoyl-sn-glycero-phosphocholine (POPC) and POPC/MGDG (monogalactosyldiacylglycerol; mole ratio 85:15) multilamellar vesicles (MLVs) to probe the peptide–lipid interaction. Solid-state ^{31}P NMR and ^{2}H NMR spectroscopic experiments revealed that the peptide perturbs the headgroup and the acyl chain regions of phospholipids as indicated by changes in spectral lineshape, chemical shift anisotropy (CSA) line width, and ^{2}H order S_{CD} parameters. In addition, the comparison between POPC MLVs and POPC/MGDG MLVs indicated that the lipid bilayer composition affected peptide perturbation of the lipids, and such perturbation appeared to be more intense in a system more closely mimicking a thylakoid membrane.

1. Introduction

In plant cells most thylakoid lumen proteins are synthesized in the cytosol as higher molecular weight precursors containing targeting sequences, which allow import into chloroplasts and localization to thylakoid lumen for function [1,2]. Two thylakoid transport systems, homologous to bacteria export systems, direct precursors to the thylakoid lumen [3]. The chloroplast Sec system transports largely *unfolded* proteins across the membrane in an ATP dependent manner, while the chloroplast twin arginine translocation (cpTat)^{2} system delivers highly *folded* proteins across the membrane utilizing the trans-thylakoidal protonmotive force as its only energy source. Another distinguishing feature of Tat transport system is the presence of a twin arginine amino acid motif in the lumen-targeting signal peptide of the precursor, which gives the pathway its name. The cpTat pathway consists of three core membrane-bound subunits, Tha4, Hcf106, and cpTatC, whereas the homologous proteins in the bacterial Tat system are TatA, TatB and TatC [2]. Sequence analysis predicts that Tha4 (TatA) and Hcf106 (TatB) have similar structure, both consisting of an N-terminal transmembrane domain (TMD), followed by an amphipathic helix (APH) and an unstructured C-terminus (C-tail) [4]; however, the APH domain and C-tail region of Hcf106 are approximately two times larger than those of Tha4. The predicted structure for Tha4 has been confirmed by determination of the structure of a truncated version of the homologous protein, $TatA_{d}$ (2–45), from *Bacillus subtilis* by solution NMR [5] and solid-state NMR [6]. Even though Tha4 and Hcf106 appear to have structural similarities, this has not been investigated directly. In addition the two proteins are functionally distinct such that one cannot functionally replace the other [4]. cpTatC is an integral membrane protein with six transmembrane-spanning helices [7,8]. Nuclear genes encode all three proteins, and they are synthesized in the cytoplasm as larger molecular weight precursors containing N-terminal amino acid extensions, the stromal-targeting transit peptides. cpTatC is localized to the thylakoid via a stromal intermediate [9], and it cannot integrate into the thylakoid membrane directly. Conversely, Tha4 and Hcf106 do not appear to use a stromal intermediate, and they can integrate directly into thylakoid membranes even in the absence of

Abbreviations: cpTat, chloroplast twin arginine transport; TMD, transmembrane domain; APH, amphipathic α-helix; POPC, 1-palmitoyl-2-oleoyl-sn-glycero-phosphocholine; MGDG, monogalactosyl diacylglycerol; MLV, multilamellar vesicles; CSA, chemical shift anisotropy; S_{CD}, segmental C–D bond order parameter

* Corresponding author at: Department of Chemistry and Biochemistry, Miami University, 651 E. High St., Oxford, OH 45056, USA. Tel.: +1 513 529 8091.
E-mail address: adabney@miamioh.edu (C. Dabney-Smith).
[1] Present address: Department of Biochemistry and Biophysics, Texas A&M University, College Station, TX 77843 USA.

0005-2736/$ – see front matter © 2013 Elsevier B.V. All rights reserved.
http://dx.doi.org/10.1016/j.bbamem.2013.10.007

their signal peptide [4]. Currently how these proteins are able to insert into the membrane spontaneously or unassisted is unknown. Here we investigated interactions of a synthetic peptide corresponding to the APH region of Hcf106 for its ability to interact with multilamellar vesicles (MLVs) as insight into the ability to spontaneously insert into thylakoid membranes. Understanding Hcf106 interaction with lipid bilayers may also provide insights into Hcf106 function and activity.

One way to better understand the integration, topology, and structure–function relationships of membrane proteins is to study the interaction between the peptide and lipids by solid-state NMR spectroscopy. Solid-state NMR techniques are widely used to study the structural and dynamic properties of peptides and lipids [10–13]. ^{31}P and ^{2}H solid-state NMR spectroscopy are useful probes to study peptide–lipid interactions from the perspective of lipids. Utilizing ^{31}P as a natural probe, which is sensitive to the conformation of lipid headgroup, lipid phase and electrostatic property, ^{31}P NMR is extensively used to investigate the dynamics and interaction between lipid headgroups with peptides [14–16]. Complementary to ^{31}P NMR, ^{2}H solid-state NMR spectroscopy provides information on the orientation and dynamics of the acyl chains of lipids by incorporating peptides or proteins into acyl-chains deuterated phospholipid bilayers [17–19]. Peptide–lipid interactions are based on the amino acid sequence of proteins and the composition of lipids, and are widely used to address questions such as protein and lipid structure, hydrophobicity and aggregation of proteins, charge distribution on lipid, depth of peptide in the lipid milieu, and modulation of interaction by altering the lipid composition [20–23]. Unlike small micelles with high curvature, which could hardly retain native structure of peptides, multilamellar vesicles (MLVs) are more membrane-mimicking systems that are composed of multi-layers of lipid bilayers [24,25].

Here we use solid-state NMR spectroscopy to investigate the topology of vesicles from the perspective of the lipids, obtaining preliminary topology information of Hcf106 in lipids by studying the peptide–lipid interaction. To simplify the study of this 176 amino acid protein, a peptide encompassing the APH (residues 28–65) of Hcf106 were synthesized by Fmoc-based solid-phase methods and purified by high-performance liquid chromatography [26]. These peptides were then incorporated into POPC (1-palmitoyl-2-oleoyl-sn-glycero-phosphoatidylcholine) and POPC/MGDG (monogalactosyldiacylglycerol) vesicles at various concentrations. The synthetic phospholipid bilayers mimicked biological membranes providing a controlled environment in which to assay peptide interaction or insertion with the membrane. A peptide from the C terminus of the small subunit of Rubisco (mSSU Rubisco) was predicted to be non-amphipathic by standard algorithms, and was used as a control peptide in this study. Using ^{31}P NMR spectroscopy we showed that Hcf106 APH peptides interact with phospholipid headgroups. In addition ^{2}H NMR spectroscopic measurements revealed the perturbation of the deuterated acyl chains by the presence of peptide and the effect of lipid composition on the peptide–lipid interaction. Further, the order parameter S_{CD} from ^{2}H NMR demonstrated the dynamic characteristics of lipid headgroup and acyl chain and the effect of peptide addition to the vesicles. These experimental results confirmed the membrane-associate activity of the proposed amphipathic helix of Hcf106 and suggested that Hcf106 mostly sat on the membrane surface and perturbed the hydrophobic region of phospholipid to a lesser extent.

2. Materials and methods

2.1. Materials

Synthetic phospholipids POPC and POPC-d_{31} were purchased from Avanti Polar Lipids (Alabaster, AL). Natural galactolipid from parsley leaves, MGDG, was purchased from Larodan Fine Chemicals AB (Sweden). All lipids were dissolved in chloroform or chloroform/methanol and stored at −20 °C under N_2 gas until use. Fmoc amino acids were purchased from Novabiochem (San Diego, CA). Peptide synthesis resin and other chemicals for synthesis were purchased from Applied Biosystems (Foster City, CA). HPLC grade acetonitrile was purchased from VWR (Radnor, PA) and was filtered through a 0.22-mm nylon membrane before use. Water was purified using a Nanopure reverse osmosis system (Millipore, Bedford, MA). Chloroform, piperidine, EDTA, N-[2-hydroxyethyl] piperazine-N″-2-ethane sulfonic acid (HEPES) and 2,2,2 trifluoroethanol (TFE) were purchased from Sigma-Aldrich (Milwaukee, WI). The deuterium-depleted water was purchased from Isotec (Miamisburg, OH).

2.2. Synthesis and purification of peptide Hcf106 APH and peptide mSSU Rubisco

Hcf106 APH and mSSU Rubisco were synthesized using Fmoc solid-phase peptide synthesize chemistry on a CEM microwave peptide synthesizer (Matthews, NC). The sequence for the amphipathic helix of Hcf106 is NH_2-LAEVARNLGKTLREFQPTIREIQDVSREFKSTLEREIG-COO^-, while the sequence for the control peptide mSSU Rubisco is NH_2-EHNKSPRYYDGRYWTMWKLPMFGTTDASQVLG-COO^-. After the peptides were cleaved from their solid support, they were purified via HPLC on a C18 reverse-phase preparation column. The column was equilibrated with 95% solvent A (100% H_2O) and 5% solvent B (60% acetonitrile, 40% H_2O for Hcf106 APH; 90% acetonitrile, 10% H_2O for mSSU Rubisco), and was eluted with a linear gradient of 5–95% solvent B. The buffers also contained 0.1% trifluoroacetic acid (TFA). The purified peptide was lyophilized to remove existing solvent. Purity was confirmed by matrix-assisted laser desorption ionization time-of-flight (MALDI-TOF) mass spectrometry to ensure the purity of the peptides.

2.3. NMR sample preparation

POPC bilayers containing Hcf106 APH peptide of various concentrations were prepared as described [15]. Briefly Hcf106 APH peptide (2.0–6.1 mg) and POPC bilayers (17.5 mg) were dissolved in 2,2,2 trifluoroethanol and chloroform, respectively, and the peptide was added to the lipids at the mol.% indicated in the figure legends. The mixtures were dried under steady N_2 gas and placed in a vacuum desiccator overnight to remove residual solvent. The multilamellar vesicles (MLVs) were prepared by suspension of the dried mixture in 95 μl HEPES buffer (30 mM HEPES, pH 7.0, 5 mM EDTA, 20 mM NaCl) followed by five cycles of moderate vortexing for 2 min, freezing with liquid N_2 for 1 min and sonication for 5 min in a 45 °C bath sonicator. While the presence of residual TFA from the cleavage reaction should be minimized, the presence of residual TFA would lower the pH of the buffer, especially given the small volume of dilute buffer added; therefore, the peptide solution may have a pH <7.0. The fully homogenized samples were transferred to NMR sample tubes. Peptide incorporation into POPC/MGDG MLVs (85%:15% ratio) were prepared following the same procedure, maintaining the total lipid amount at 17.5 mg. For the ^{2}H NMR experiments, 5 mg POPC-d_{31} phospholipids replaced the same amount of non-deuterated POPC in the sample to maintain total lipid amount (17.5 mg). POPC and POPC/MGDG MLVs containing 6 mol.% control peptide from the SSU of Rubisco (5.3 mg) were prepared by the same procedure.

2.4. NMR spectroscopy

All NMR data were recorded on a Bruker Avance 500 MHz WB NMR spectrometer equipped with a CPMAS probe (Bruker, Billerica, MA). ^{31}P NMR spectra were acquired at 202.4 MHz with proton decoupling using a 4 μs 90° pulse and a 4 s recycle delay. For the ^{31}P static NMR spectra 512 scans were taken and the free induction delay was processed using 200 Hz of line broadening. The spectral width was set to 500 ppm. All ^{31}P NMR spectra were referenced by assigning the 85% H_3PO_4 ^{31}P peak to 0 ppm.

^{2}H NMR spectra were performed at 76.77 MHz employing a quadrupolar echo pulse sequence using quadrature detection with complete phase cycling of the pulse pairs. The 90° pulse length was 4 μs, the interpulse delay was 40 μs, the recycle delay was 0.4 s, and the spectral width was set to 100 kHz. For the ^{2}H static NMR spectra 122,880 scans were taken and were processed using 200 Hz of line broadening. Powder-type ^{2}H NMR spectra were deconvoluted (dePaked) using the algorithm of McCabe and Wassall [27] such that the bilayer normal was perpendicular with respect to the direction of the static magnetic field. The quadrupolar splittings were measured from the dePaked spectra, and the ^{2}H order parameters S_{CD} were calculated according to the equation $S_{CD}^i = \Delta\nu_i/(3/2(e^2qQ/h))$, where S_{CD}^i is the quadrupolar splitting for a deuteron attached to the ith carbon of the POPC acyl chain, and e^2qQ/h is the quadruple coupling constant (168 kHz for deuteron in C–D bonds). The order parameters of the methyl groups at the terminal acyl chain were multiplied by three as the calculated values [28].

3. Results and discussion

3.1. ^{31}P NMR studies indicate Hcf106 APH interaction with MLVs

Chloroplast Tat component Hcf106 is predicted to contain an N-terminal proximal amphipathic α-helix (Fig. 1A), which has not been characterized experimentally. In addition, previous studies suggest that Hcf106 has the ability to insert into the thylakoid via the spontaneous pathway, requiring no membrane bound protein assistance or additional energy, either in the form of nucleotide triphosphate hydrolysis or transmembrane protonmotive force [4]. To better understand the ability of Hcf106 to interact with membranes, we investigated the membrane interactivity of one of the key predicted membrane active components, the APH, using a synthetic peptide (Fig. 1A). Helical wheel projections of the APH peptide used in this study clearly indicate the presence of a hydrophilic face and a hydrophobic face of the helix (Fig. 1B).

To investigate the nature of lamellar and nonlamellar phase transitions exhibited by the POPC MLVs in the presence of the Hcf106 APH peptide, static ^{31}P NMR spectroscopic measurements were made (Fig. 2A). The Hcf106 APH peptide concentration was varied from 0 to 6 mol.% with respect to POPC lipids. As expected for POPC bilayers at a temperature above the chain melting transition temperature (T_m) of −2 °C [29], all spectra displayed a motionally averaged powder-pattern at 25 °C, indicating that the phospholipid bilayers are in the liquid crystalline phase (Fig. 2A). Increasing amounts of Hcf106 APH peptide incorporated into POPC MLVs caused a corresponding increase in the static lineshape width of the ^{31}P NMR spectra as compared to the lineshape width of the empty POPC vesicles (Fig. 2A). Furthermore, the addition of the peptide caused a corresponding decrease in the chemical shift anisotropy (CSA, $\sigma_{\|} - \sigma_{\perp}$) line widths. CSA line widths were measured for control vesicles and vesicles containing 6 mol.% APH peptide (Fig. 2A) and were found to be 45 ± 1 ppm and 42 ± 1 ppm, respectively. There was a 3 ppm decrease in CSA line width when 6 mol.% peptide was added as compared to control POPC bilayers, indicating that the headgroup region of the phospholipid bilayer was perturbed by the addition of Hcf106 APH peptide. This change contrasts directly with a CSA line width measure of 45 ± 1 ppm in the presence of 6 mol.% control peptide (Supplemental Fig. 1A), which was indistinguishable from control vesicles.

The Hcf106 APH peptide is derived from the thylakoid localized Hcf106 protein. Thylakoid membrane has a very high proportion of nonphospholipids to phospholipids as well as a high proportion of the nonbilayer forming lipid, monogalactosyl diacylglycerol (MGDG) that can compose >50% of thylakoid lipid [30]. To more closely mimic the native thylakoid lipid composition, we tested Hcf106 APH interaction with vesicles containing 15 mol.% MGDG. In this synthetic system, we were able to easily generate vesicles containing 15 mol.% MGDG (85:15 mole ratio POPC:MGDG), but higher concentrations yielded unstable vesicles and were not used for this study. When increasing amounts of the Hcf106 APH peptide were incorporated into POPC/MGDG MLVs, the corresponding ^{31}P lineshape broadened compared to that of control POPC/MGDG MLVs (Fig. 2B). As with POPC MLVs, the CSA widths decreased as more peptide was added to the POPC/MGDG MLVs.

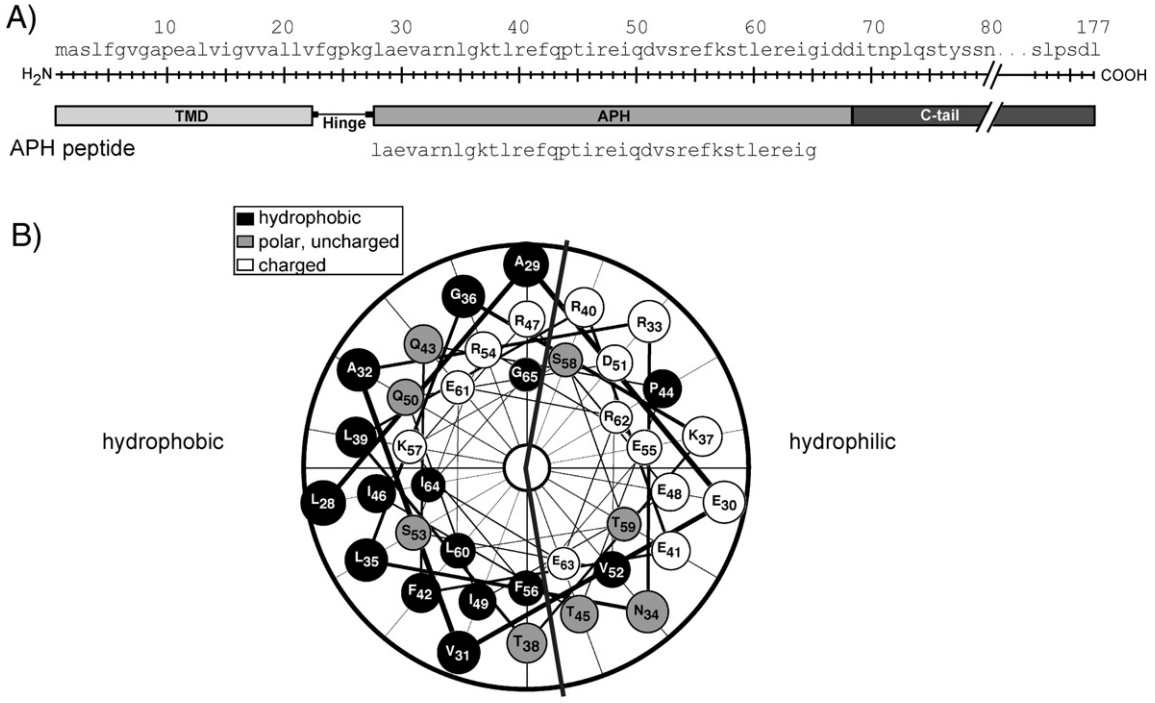

Fig. 1. Schematic of Hcf106 and peptide used in this study. Peptides were synthesized on a CEM microwave peptide synthesizer (Matthews, NC) using Fmoc solid-phase peptide synthesis chemistry as described in Materials and Methods. (A) A schematic of Hcf106 showing the different domains. The amino acid sequence of the peptide representing the APH is indicated. (B) Helical wheel plot (DNAStar, Madison, WI) of the amino acids of the Hcf106 APH peptide indicating the hydrophilic and hydrophobic faces.

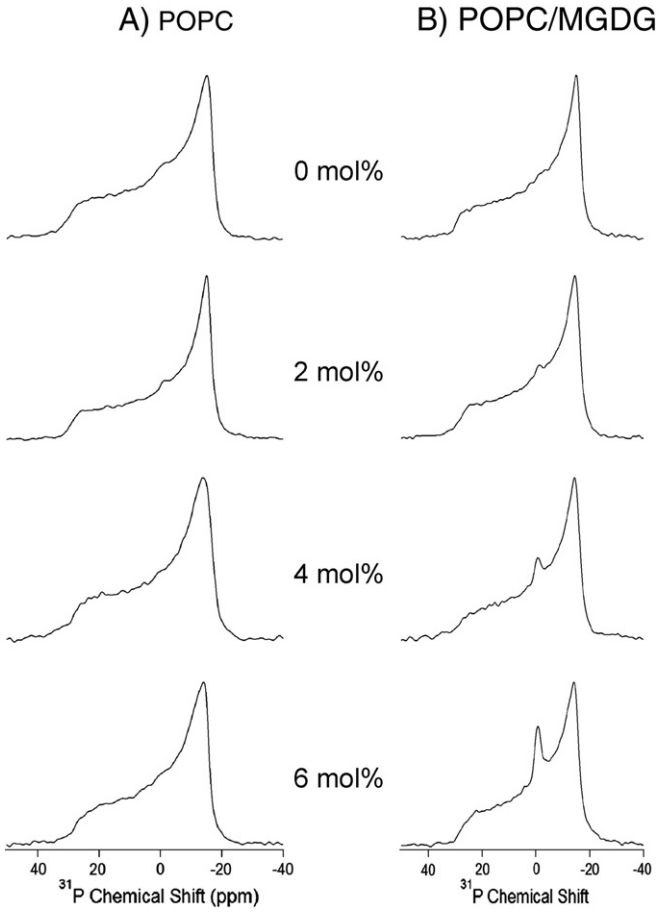

Fig. 2. Hcf106 APH preferentially perturbs POPC/MGDG MLVs. (A) ^{31}P spectra of MLV samples showing the effect of Hcf106 APH on ^{31}P spectra line shape of POPC bilayers as a function of Hcf106 APH peptide concentration. (B) ^{31}P spectra of MLV samples showing the effect of Hcf106 APH on ^{31}P spectra line shape of POPC/MGDG bilayers (85%:15%) as a function of Hcf106 APH concentration at 25 °C. MLV samples of different lipids in the absence of Hcf106 APH, and in the presence of 2, 4, and 6 mol.% Hcf106 APH with respect to lipids were investigated.

The CSA widths for control POPC/MGDG MLVs and MLVs containing 6 mol.% APH peptide were 45 and 41 ppm, respectively. There was a 4 ppm decrease in CSA width when 6 mol.% peptide was added when compared to the empty vesicles. However the presence of the control peptide with POPC/MGDG vesicles resulted in a CSA line width of 45 ± 1 ppm, the same as control vesicles (Supplemental Fig. 1B). The most obvious difference in ^{31}P spectra lineshape between the POPC MLVs and the POPC/MGDG MLVs was the appearance of an isotropic peak that increased in intensity as the concentration of Hcf106 APH was increased (Fig. 2B). The presence of such an isotropic peak suggests that smaller vesicles were induced to form due to the presence of the APH peptides and the contribution from the isotropic phase increased as more Hcf106 APH was incorporated [31].

At least three possible occurrences can explain this change in CSA line width: (1) increased stochastic fluctuations experienced by the lipid head groups due to an increase in the disorder of individual lipids caused by the increasing presence of the APH, but not the control, peptide; (2) increased axial rotational motion as well as lateral diffusion rate of lipid upon peptide incorporation; or (3) increased dynamics of the vesicles, resulting from the interaction between the peptide and head groups of the phospholipids [13,32–34]. However, an increase in the long axis rotation of the lipid would be unlikely to affect the CSA line width because at the point at which the ^{31}P CSA line width becomes axially symmetric it has reached an average and increasing the rotation at that point will not change those averages. In addition, an increase in the lateral diffusion rate of the lipid is also unlikely to be large enough to affect the CSA line width. More likely the change in CSA line width is due to an increase in the disorder of the individual lipids as the amount of the APH, but not the control, peptide increases. For example, a decrease in the CSA line width may correspond to a change in the orientation of the head groups of the lipid such that they are less upright (i.e., the angle ϑ_x of the chemical shift tensor increases from the lipid axis of rotation perpendicular to the plane of the phosphorous and oxygens [35]). Regardless, the shift in CSA when the APH peptide was present indicates a perturbation of the liquid crystalline array of the lipids, and a change in averaged orientation of the lipid head groups with respect to the bilayer normal, induced by rotational motion of lipid head group [32,36]. Regardless, the APH peptide interacted with MLVs containing the thylakoid-specific lipid, MGDG, more intensely as compared to MLVs containing only POPC.

3.2. ^{2}H NMR studies indicate perturbation of POPC and POPC/MGDG lipids acyl chain upon Hcf106 APH incorporation

Because static ^{31}P NMR spectra only reflect the perturbation of the peptide to the phospholipid headgroup, ^{2}H solid-state NMR spectroscopy was utilized to investigate the effect of increasing concentration of Hcf106 APH peptide on the order and dynamics of the acyl chain of POPC-d_{31} phospholipid in POPC and POPC/MGDG MLVs (Fig. 3). All spectra display

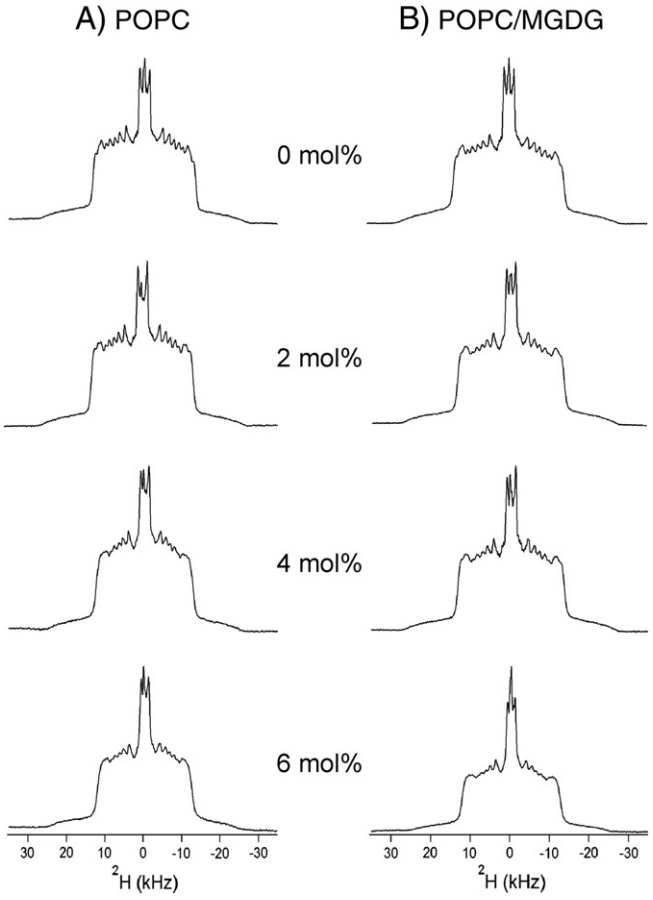

Fig. 3. Hcf106 APH interacts with the bilayer of POPC or POPC/MGDG MLVs. ^{2}H NMR spectra of MLV samples showing the perturbation of Hcf106 APH on lipids acyl chain of (A) POPC bilayers, and (B) POPC/MGDG bilayers as a function of Hcf106 APH concentration at 25 °C. POPC-d_{31} phospholipids (5 mg) were used as deuterium probe. MLV samples of different lipids in the absence of Hcf106 APH, and in the presence of 2, 4, and 6 mol.% Hcf106 APH with respect to lipids were investigated.

overlapping doublet resonances with the largest splitting resulting from the C–D bond closest to the glycerol backbone and the central splitting arising from the terminal methyl group [13,31,34]. Clearly, addition of APH peptide at various concentrations altered the line shape and resolution of ^{2}H NMR spectra of the POPC/POPC-d_{31} MLVs significantly compared to the control sample lacking peptide (Fig. 3A). The spectral widths decreased upon addition of the APH peptide, indicating an increase in the lipid bilayer fluidity caused by perturbation of lipid acyl chains upon peptide incorporation. As the concentration of APH peptide increased there was a loss of resolution of the spectrum as demonstrated by the disappearance of sharp edges of the peaks, also revealing an interaction between the APH peptide and the acyl chains of the lipid bilayer. In addition, this interaction increased the motion of the lipids and/or the dynamics of the vesicles, as evidenced by the increased isotropic peak intensity induced by higher amounts of APH peptide. Similar to the presence of an isotropic peak in the ^{31}P NMR measurements, the increased dynamics of the vesicles could be explained by the formation of small, rapidly tumbling vesicles [31]. The spectral line shape and isotropic component was even more pronounced when Hcf106 APH peptides were added to POPC/POPC-d_{31}/MGDG MLVs (Fig. 3B). In contrast the line shape widths of the MLVs (either POPC/POPC-d_{31} or POPC/POPC-d_{31}/MGDG) were not changed from those of the control vesicles when in the presence of the control peptide (Supplemental Fig. 2), although the presence of the control peptide did cause the formation of an isotropic peak. Taken with the static ^{31}P NMR data, these data indicate that the Hcf106 peptide interacts with the POPC/MGDG vesicles, and does so in the same way as it interacts with the POPC vesicles.

However the changes in CSA line widths and in the ^{2}H NMR spectral line shapes due to the presence of the peptide were not very large (barely 10% change) and may be a reflection of how the peptide can engage the membrane. In vesicles containing the thylakoid-specific lipid, the APH peptide may be a membrane breaching peptide at high enough concentrations, similar to antimicrobial peptides, and this is evidenced by the increasing presence of the isotropic peak with increasing peptide amount. The presence of the MGDG lipid may enhance the membrane breaching capabilities of the APH peptide due to its tendency to not form a lamellar bilayer but rather to form a nonlamellar, inverted Hexagonal (Hexagonal II) phase.

All ^{2}H NMR powder pattern spectra were dePaked to probe the dynamic changes of the acyl chains upon Hcf106 APH peptide incorporation. S_{CD} order parameters are sensitive to intermolecular, intramolecular and collective motions, reflecting the orientation and dynamic change of the C–D bond vector [37,38]. The smoothed segmental C–D bond order parameters (S_{CD}) were calculated from the dePaked spectra and plotted as a function of acyl chain carbon number for the different APH concentration at 25 °C (Fig. 4). As distance from the glycerol backbone increased, there was a decrease of S_{CD} for all samples, indicating increased motion and flexibility for the central and terminal acyl chain regions as compared to the proximal headgroup region (Fig. 4A, filled circles). In the presence of 2, 4 and 6 mol.% APH peptides, the acyl chains of POPC lipid bilayers were more mobile compared to the control vesicles lacking peptide or vesicles containing the control peptide, as revealed by a decrease in the order of each C–D bond (Fig. 4A). In the presence of the APH peptide, there was a larger decrease in the S_{CD} for the first three or four carbons from the ester than at the methyl end of the acyl chains (Fig. 4A). Combined with the ^{31}P NMR data, these data suggest that Hcf106 APH peptide mostly sits on the membrane surface or may slightly tilt into the hydrophobic region of the phospholipid bilayers to interact with acyl chains in close proximity to glycerol backbones. It is also possible that Hcf106 APH peptide attached to the membrane surface by its hydrophilic face and induced a relatively compact environment on the membrane surface and more dynamic space in the hydrophobic region of the lipids. Further experiments are needed to verify these explanations. The S_{CD} profile for POPC/MGDG MLVs (Fig. 4B) resembles that in POPC MLVs, except

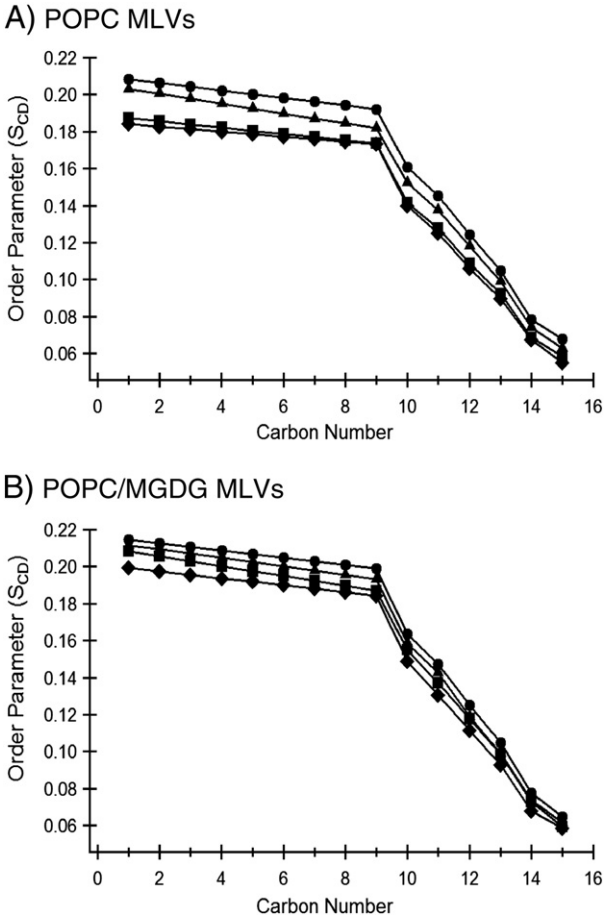

Fig. 4. Hcf106 APH preferentially disturbs the lipid head group/acyl chain interface. Smoothed acyl chains orientational order S_{CD} profiles calculated by DePaking ^{2}H NMR spectra of Fig. 3. POPC MLVs (A) and POPC/MGDG MLVs (B) with and without Hcf106 APH at various concentrations. S_{CD} profiles calculated in the absence (●) or presence of Hcf106 APH at 2 mol.% (▲), 4 mol.% (■) and 6 mol.% (◆), respectively.

that POPC MLVs demonstrate a slightly larger S_{CD} and less perturbation caused by the incorporation of Hcf106 APH peptide.

4. Conclusion

This solid-state NMR study clearly shows lipid–peptide interaction. ^{31}P and ^{2}H solid-state NMR static spectra lineshape, CSA widths, and ^{2}H order parameters are utilized to investigate lipid–peptide interaction and the results are complimentary to each other. These data indicate that Hcf106 APH peptide interacts with the head group and acyl chains of phospholipid bilayers. The manipulation of the lipid composition clearly alters the line shape of the spectra, and the peptides interact more intensely with the thylakoid membrane-mimicking environment (POPC/MGDG MLVs). These data show for the first time that Hcf106 APH is by itself a membrane associated peptide, and also imply how the peptide could arrange itself to interact with lipids when incorporated into membrane systems.

Supplementary data to this article can be found online at http://dx.doi.org/10.1016/j.bbamem.2013.10.007.

Acknowledgements

This work was funded by the DOE Office of Science Early Career Research Program grant (DE-FG02-10ER16138 to CDS) through the Office of Basic Energy Sciences and National Institutes of Health grant (R01GM080542 and GM080542Z to GAL).

References

[1] L.X. Shi, S.M. Theg, The chloroplast protein import system: from algae to trees, BBA Mol. Cell Res. 1833 (2013) 314–331.
[2] J.M. Celedon, K. Cline, Intra-plastid protein trafficking: how plant cells adapted prokaryotic mechanisms to the eukaryotic condition, BBA Mol. Cell Res. 1833 (2013) 341–351.
[3] K. Cline, C. Dabney-Smith, Plastid protein import and sorting: different paths to the same compartments, Curr. Opin. Plant Biol. 11 (2008) 585–592.
[4] V. Fincher, C. Dabney-Smith, K. Cline, Functional assembly of thylakoid deltapH-dependent/Tat protein transport pathway components in vitro, Eur. J. Biochem. 270 (2003) 4930–4941.
[5] Y. Hu, E. Zhao, H. Li, B. Xia, C. Jin, Solution NMR structure of the TatA component of the twin-arginine protein transport system from gram-positive bacterium Bacillus subtilis, J. Am. Chem. Soc. 132 (2010) 15942–15944.
[6] T.H. Walther, S.L. Grage, N. Roth, A.S. Ulrich, Membrane alignment of the pore-forming component TatA(d) of the twin-arginine translocase from Bacillus subtilis resolved by solid-state NMR spectroscopy, J. Am. Chem. Soc. 132 (2010) 15945–15956.
[7] H. Mori, E.J. Summer, K. Cline, Chloroplast TatC plays a direct role in thylakoid (Delta)pH-dependent protein transport, FEBS Lett. 501 (2001) 65–68.
[8] S.E. Rollauer, M.J. Tarry, J.E. Graham, M. Jaaskelainen, F. Jager, S. Johnson, M. Krehenbrink, S.M. Liu, M.J. Lukey, J. Marcoux, M.A. McDowell, F. Rodriguez, P. Roversi, P.J. Stansfeld, C.V. Robinson, M.S. Sansom, T. Palmer, M. Hogbom, B.C. Berks, S.M. Lea, Structure of the TatC core of the twin-arginine protein transport system, Nature 492 (2012) 210–214.
[9] J.R. Martin, J.H. Harwood, M. McCaffery, D.E. Fernandez, K. Cline, Localization and integration of thylakoid protein translocase subunit cpTatC, Plant J. 58 (2009) 831–842.
[10] T.A. Cross, S.J. Opella, Solid-state NMR structural studies of peptides and proteins in membranes, Curr. Opin. Struct. Biol. 4 (1994) 574–581.
[11] Y. Nakazawa, T. Asakura, Structure determination of a peptide model of the repeated helical domain in Samia cynthia ricini silk fibroin before spinning by a combination of advanced solid-state NMR methods, J. Am. Chem. Soc. 125 (2003) 7230–7237.
[12] A. Watts, Solid-state NMR approaches for studying the interaction of peptides and proteins with membranes, Biochim. Biophys. Acta 1376 (1998) 297–318.
[13] S. Abu-Baker, G.A. Lorigan, Phospholamban and its phosphorylated form interact differently with lipid bilayers: a 31P, 2H, and 13C solid-state NMR spectroscopic study, Biochemistry 45 (2006) 13312–13322.
[14] I.C.P. Smith, I.H. Ekiel, Phosphorus-31 NMR of membranes, in: D.G. Gorenstein (Ed.), Phosphorus-31 NMR: principles and applications, Academic Press, Orlando, Fla., 1984, pp. 447–475.
[15] P.C. Dave, E.K. Tiburu, K. Damodaran, G.A. Lorigan, 31P and 2H solid-state NMR spectroscopic studies of the transmembrane domain of the membrane-bound protein phospholamban, Biophys. J. 86 (2004) 1564–1573.
[16] J.S. Santos, D.K. Lee, A. Ramamoorthy, Effects of antidepressants on the conformation of phospholipid headgroups studied by solid-state NMR, Magn. Reson. Chem. 42 (2004) 105–114.
[17] B.W. Koenig, J.A. Ferretti, K. Gawrisch, Site-specific deuterium order parameters and membrane-bound behavior of a peptide fragment from the intracellular domain of HIV-1 gp41, Biochemistry 38 (1999) 6327–6334.
[18] S. Yamaguchi, D. Huster, A. Waring, R.I. Lehrer, W. Kearney, B.F. Tack, M. Hong, Orientation and dynamics of an antimicrobial peptide in the lipid bilayer by solid-state NMR spectroscopy, Biophys. J. 81 (2001) 2203–2214.
[19] J.X. Lu, K. Damodaran, J. Blazyk, G.A. Lorigan, Solid-state nuclear magnetic resonance relaxation studies of the interaction mechanism of antimicrobial peptides with phospholipid bilayer membranes, Biochemistry 44 (2005) 10208–10217.
[20] A. Arora, L.K. Tamm, Biophysical approaches to membrane protein structure determination, Curr. Opin. Struct. Biol. 11 (2001) 540–547.
[21] A. Watts, Protein–lipid interactions: do the spectroscopists now agree? Nature 294 (1981) 512–513.
[22] M.A. Lemmon, D.M. Engelman, Specificity and promiscuity in membrane helix interactions, FEBS Lett. 346 (1994) 17–20.
[23] M. Bloom, E. Evans, O.G. Mouritsen, Physical properties of the fluid lipid-bilayer component of cell membranes: a perspective, Q. Rev. Biophys. 24 (1991) 293–397.
[24] A. Jesorka, O. Orwar, Liposomes: technologies and analytical applications, Annu Rev Anal Chem (Palo Alto, Calif) 1 (2008) 801–832.
[25] G.W. Stockton, C.F. Polnaszek, A.P. Tulloch, F. Hasan, I.C. Smith, Molecular motion and order in single-bilayer vesicles and multilamellar dispersions of egg lecithin and lecithin-cholesterol mixtures. A deuterium nuclear magnetic resonance study of specifically labeled lipids, Biochemistry 15 (1976) 954–966.
[26] E.K. Tiburu, P.C. Dave, J.F. Vanlerberghe, T.B. Cardon, R.E. Minto, G.A. Lorigan, An improved synthetic and purification procedure for the hydrophobic segment of the transmembrane peptide phospholamban, Anal. Biochem. 318 (2003) 146–151.
[27] M.A. Mccabe, S.R. Wassall, Fast-Fourier-transform DePaking, J. Magn. Reson. Ser. B 106 (1995) 80–82.
[28] J.-X. Lu, M.A. Caporini, G.A. Lorigan, The effects of cholesterol on magnetically aligned phospholipid bilayers: a solid-state NMR and EPR spectroscopy study, J. Magn. Reson. 168 (2004) 18–30.
[29] J. Seelig, 31P nuclear magnetic resonance and the head group structure of phospholipids in membranes, Biochim. Biophys. Acta 515 (1978) 105–140.
[30] R. Douce, J. Joyard, Biochemistry and function of the plastid envelope, Annu. Rev. Cell Biol. 6 (1990) 173–216.
[31] P.C. Dave, E.K. Tiburu, K. Damodaran, G.A. Lorigan, Investigating structural changes in the lipid bilayer upon insertion of the transmembrane domain of the membrane-bound protein phospholamban utilizing P-31 and H-2 solid-state NMR spectroscopy, Biophys. J. 86 (2004) 1564–1573.
[32] S.J. Kohler, M.P. Klein, Orientation and dynamics of phospholipid head groups in bilayers and membranes determined from P-31 nuclear magnetic-resonance chemical shielding tensors, Biochemistry 16 (1977) 519–526.
[33] S. Abu-Baker, X. Qi, J. Newstadt, G.A. Lorigan, Structural changes in a binary mixed phospholipid bilayer of DOPG and DOPS upon saposin C interaction at acidic pH utilizing 31P and 2H solid-state NMR spectroscopy, Biochim. Biophys. Acta 1717 (2005) 58–66.
[34] J.X. Lu, K. Damodaran, G.A. Lorigan, Probing membrane topology by high-resolution 1H-13C heteronuclear dipolar solid-state NMR spectroscopy, J. Magn. Reson. 178 (2006) 283–287.
[35] J.D. Gehman, C.C. O'Brien, F. Shabanpoor, J.D. Wade, F. Separovic, Metal effects on the membrane interactions of amyloid-beta peptides, Eur. Biophys. J. 37 (2008) 333–344.
[36] R.G. Griffin, L. Powers, P.S. Pershan, Head-group conformation in phospholipids - P-31 nuclear magnetic-resonance study of oriented monodomain dipalmitoylphosphatidylcholine bilayers, Biochemistry 17 (1978) 2718–2722.
[37] A. Seelig, J. Seelig, The dynamic structure of fatty acyl chains in a phospholipid bilayer measured by deuterium magnetic resonance, Biochemistry 13 (1974) 4839–4845.
[38] J. Seelig, A. Seelig, Deuterium magnetic resonance studies of phospholipid bilayers, Biochem. Biophys. Res. Commun. 57 (1974) 406–411.